Quaternary International 275 (2012) 14–22

Contents lists available at SciVerse ScienceDirect

Quaternary International

journal homepage: www.elsevier.com/locate/quaint

Assessing post-depositional processes in archaeological cave fires through the analysis of archaeomagnetic vectors

Á. Carrancho [a,b,*], J.J. Villalaín [a], J.M. Vergès [c], J. Vallverdú [c]

[a] Dpto. Física, Universidad de Burgos, Escuela Politécnica Superior, Avda. Cantabria S/N, 09006 Burgos, Spain
[b] National Research Center on Human Evolution (CENIEH), Avenida Sierra de Atapuerca, s/n, 09002 Burgos, Spain
[c] Institut Català de Paleoecologia Humana i Evolució Social (IPHES) – Àrea de Prehistòria, Universitat Rovira i Virgili, Pl. Imperial Tarraco, 1, 43005 Tarragona, Spain

ARTICLE INFO

Article history:
Available online 16 January 2012

ABSTRACT

This paper presents a methodological application of archaeomagnetism and rock-magnetism as a tool to evaluate post-depositional mechanical alterations in archaeological cave fires. Most taphonomic and post-depositional studies on anthropogenic sediments have mainly focused on the diagenetic alterations that these contexts undergo from a geochemical point of view. However, physical alterations are still largely assessed from mere macroscopic observations of the burnt facies comprising these fires. This paper compares the archaeomagnetic directions recorded in the ashes of two Holocene fires from the Mirador Cave (Sierra de Atapuerca, Burgos, Spain), one apparently well-preserved and the other clearly bioturbated. Vector analyses of archaeomagnetic directions, together with the study of magnetic properties combined with field (macroscopic) observations, can provide a powerful tool to assess when a fire is actually *in situ*. The anisotropy of magnetic susceptibility (AMS) in both fires exhibits a dominant sedimentary fabric produced by compaction, and also exhibits differences between the areas mechanically disturbed within these fires from those which are not. The following set of magnetic features was identified when an archaeological fire preserves its primary position: *i)* univectoral and high intensity NRM orthogonal demagnetisation diagrams in ashes, *ii)* Koenigsberger (Q_n) ratio values higher than unity indicative of an undisturbed thermo-remanence (TRM) or a partial-thermoremanence (p-TRM) and *iii)* a good clustering of characteristic directions defining an statistically representative mean archaeomagnetic direction. The concurrence of these observations can be used as criterion to determine when an archaeological cave fire is physically *in situ*, thus allowing a correct interpretation of the archaeological record.

1. Introduction

Determine whether an archaeological feature is *in situ* or not is a key aspect in the interpretation of the occupation of archaeological sites and cave deposits. The correct interpretation of the type, nature and duration of human occupations depends largely on the proper preservation of the (geo)archaeological record. Once deposited, both the archaeological remains and the surrounding sediments can undergo multiple syndepositional and post-depositional processes related to anthropogenic, geogenic and biogenic activity (Goldberg and Sherwood, 2006). These secondary processes include physical alterations that can lead to mechanical reorganization of the sediments (e.g., trampling, digging, burrowing) and/or chemical alterations (e.g., diagenesis and mineralogical transformations). Responsible agents may be human/biological or natural in origin and depending on the degree of impact, the integrity of the archaeological record can be severely affected and therefore its interpretation.

The study of site formation and post-depositional processes at archaeological sites have been traditionally addressed with standard sedimentological techniques to bulk samples including grain size and compositional analysis, pH, calcium carbonate or organic matter contents, among others (e.g., Bonifay, 1956; Farrand, 1975). More recently, others analytical techniques such as soil micromorphology, scanning electron microscopy (SEM), X-ray analyses (e.g., microprobe and X-ray diffraction), and Fourier Transform Infrared spectrometry (FTIR) have been extensively employed in studies of mineral diagenesis, bone preservation or evolution of the sediments at many sites worldwide (e.g., Weiner et al., 1993, 2002, 2007; Shahack-Gross et al., 2003; Karkanas, 2010). The potential of these techniques with regard to post-depositional processes at archaeological sites is indisputable and have expanded over time as new analytical techniques have become available.

Magnetic methods represent one of the most versatile techniques applied to archaeology, increasingly used in recent years to

* Corresponding author. Dpto. Física, Universidad de Burgos, Escuela Politécnica Superior, Avda. Cantabria S/N, 09006 Burgos, Spain.
E-mail address: acarrancho@ubu.es (Á. Carrancho).

1040-6182/$ – see front matter © 2012 Elsevier Ltd and INQUA. All rights reserved.
doi:10.1016/j.quaint.2012.01.010

the study of a variety of questions. The most widely known use of Archaeomagnetism is dating, but other archaeological applications of mineral magnetic methods include sediment sourcing, fire identification, palaeoenviromental reconstruction or spatial patterning analysis (e.g., Lanos et al., 1999; Herries, 2009; Herries and Fisher, 2010). This paper deals with the application of magnetic methods to the identification and study of post-depositional processes undergone by archaeological cave fires.

Two different Holocene fires from the Mirador Cave (Sierra de Atapuerca, Burgos, Spain) were studied, one apparently *in situ* and the other clearly affected by bioturbation. The identification of post-depositional movements could not be obvious due to the nature of these contexts. Vector analysis of archaeomagnetic samples can be a useful tool in order to determine if post-depositional movements have taken place after the acquisition of a stable and homogeneous magnetisation as a thermo-remanent magnetisation (TRM) in archaeological fires. Results are presented by comparing the archaeomagnetic directions obtained on both structures together with other magnetic properties. The goals of this paper are to: i) evaluate the *in situ* character of archaeological cave fires beyond macroscopic observations determined in the field, ii) determine to what extent has been reworked an archaeological fire by physical (mechanical) alteration processes; and iii) establish magnetic criterion in order to assess post-depositional processes in archaeological cave fires, with particular interest in anthropogenic sediments.

2. Archaeological context and sampled materials

Mirador Cave (42 °20′ 58″ N, 03° 30′ 33″ W) is located in the southern slope of the Sierra de Atapuerca, 15 km east of the city of Burgos (North-Central Spain; Fig. 1). This cave forms part of the karst system where several archaeological and palaeontological sites have documented human occupations from the Early Pleistocene to the Holocene (e.g.: Arsuaga et al., 1997; Bermúdez de Castro et al., 1999; Carbonell et al., 2008). Archaeological field-work at the Mirador Cave began in 1999 through a 6 m^2 survey pit, with the aim of collecting archaeological and paleoenvironmental data in order to design a reference sequence of the site. To date, the stratigraphic sequence documented comprises levels from the Uppermost Pleistocene to the Holocene.

The interest for this study resides in the Holocene series which approximately has 5.5 m thickness and consists of 25 archaeological units ranging from Neolithic to Bronze Ages (Vergés et al., 2002, 2008). A peculiarity of the Holocene series is the notable presence of ash lenses exposed along the stratigraphy, produced by the periodic combustion of domestic livestock dung, mainly sheep and goats. These anthropogenic sequences are known in the archaeological literature as *fumiers* and consist of alternating burnt dung layers with unburnt dung levels. By burning, the caves were cleaned from parasites due to livestock penning, a common practice that is widely reported along the Mediterranean region (Brochier, 1983; Brochier et al., 1992; Boschian, 1997; Boschian and Montagnari-Kokelj, 2000; Karkanas, 2006; Polo Díaz and Fernández Eraso, 2010).

The Holocene archaeological record of the Mirador Cave, with Neolithic and Bronze Age levels, is especially rich in paleobotanical and faunal remains, as well as other elements such as pottery fragments and lithic artefacts (Vergés et al., 2002, 2008; Martín et al., 2009). The anthropogenic origin of the Holocene sequence and its primary use as a cave fold is not only supported by the archaeological finds, but also by the archaeobotanical and mineral composition of the sediment (Angelucci et al., 2009; Cabanes et al., 2009). Noteworthy is the existence of a collective human burial with signs of canibalism identified at the Bronze levels, indicating that the site also had a sepulchral use (Cáceres et al., 2009). Sedimentological, stratigraphic and chronological details have been reported elsewhere (Vergés et al., 2002, 2008).

The materials reported here correspond with two different *fumiers* (ash-rubefaction couplets). The first (FU1 —Unit Mir12—) is exposed on the west section of the survey pit and contains a ~10-cm thick layer of white ash over a 2 cm rubefacted facies. It does not display any evidence of post-depositional physical disturbance, so apparently it is well-preserved (Fig. 2a). The presence of the rubefaction underlying all the length of the ashes is considered to be a good indicator of the fire preservation. The second *fumier* studied (BR1 —Unit Mir4) corresponds to the Late Bronze Age, and is exposed on the east section of the survey pit. It also contains 15–20 cm of ashes over a discontinuous and poorly defined rubefacted facies. The most important feature of this fire and the reason for sampling it is that is clearly cut by a burrow in its middle part (Fig. 2b). The heterogeneous texture and grey-brownish ashes suggest that most have been reworked.

There is not direct dating for stratigraphic unit Mir12 where the *fumier* FU1 is located. However, its maximum and minimum age can be determined by the dates from the upper and lower units whose ages are quite similar: 5360 ± 50 ^{14}C BP (Unit Mir11; 4330–4040 cal B.C.) and 5470 ± 40 ^{14}C BP (Unit Mir13;

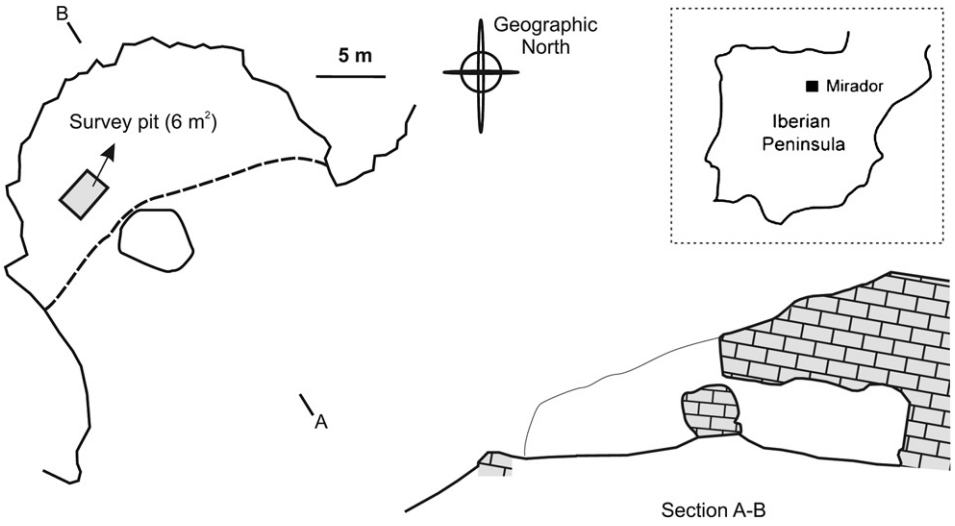

Fig. 1. Plan and section view of Mirador Cave showing the location of the 6 m^2 survey pit and location of the site.

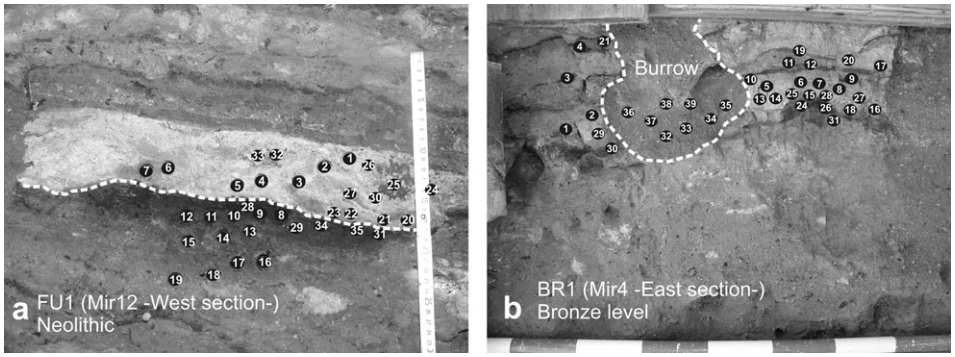

Fig. 2. (a–b) The two fires sampled indicating the location of the oriented specimens. The alteration surface created by a burrow in the right figure is indicated by a dotted line. The dotted line in the left figure indicates the contact between the ash and rubefacted facies.

4360–4240 cal B.C.), respectively. Bioturbated *fumier* BR1 corresponds with the unit Mir4. Two different dates are available for this unit, one at the top with 3040 ± 40 ^{14}C BP (Mir4 top; 1400–1190 cal B.C.) and another at the base with 3400 ± 40 ^{14}C BP (Mir4 base; 1760–1610 cal B.C.). The ages have been determined through AMS radiocarbon dates on fragments of charred wood and charred seed. The age ranges provided are the 2δ range and were calibrated with the program CALIB 5.0.2 (Stuiver et al., 2005). For further details on the dating, the reader is referred to Vergès et al. (2008).

3. Materials and methods

3.1. Archaeomagnetic sampling

A total of 72 oriented archaeomagnetic samples were taken from both burning features (*fumiers*), 39 samples from *fumier* BR1, including 8 samples from the burrow, and another 33 from FU1, with 18 samples corresponding to pure white to grey ash (Fig. 2). Sampling was carried out by means of a non-magnetic cylindrical piston specially designed for soft lithologies and incorporating a built-in orientation system. Each sample was contained in cylindrical plastic capsules (Ø 16.5 mm, length 17 mm; 3.6 cm^3) and stored in cold conditions (~3 °C) to avoid chemical alterations. Two ash samples of each *fumier* were injected by the same means into plaster capsules for thermal demagnetisation of the natural remanent magnetisation (NRM). The magnetisation of the plaster recipient is negligible compared to the magnetisation of the archaeological samples (around two orders of magnitude lesser). The plaster samples were impregnated with a solution of sodium silicate (*waterglass*) to consolidate them.

3.2. Experimental methods

All the experiments reported here have been carried out at the laboratory of palaeomagnetism of Burgos University (Spain). The measurement of the natural remanent magnetisation (NRM) was carried out with a cryogenic magnetometer 2G (noise level 5×10^{-12} Am^2). The low-field magnetic susceptibility (MS) and its anisotropy (AMS) were measured at room temperature with a KLY-4 susceptometer (AGICO, noise level 3×10^{-8} S.I.). The NRM stability was analysed by stepwise progressive alternating field (AF) and thermal demagnetisation. AF demagnetisation was carried out in 16 steps up to a maximum peak field of 100 mT with a 2G600 automatic sample degaussing system. Thermal demagnetisation was performed in 16 steps until temperatures of 620–640 °C using a TD48-SC (ASC) thermal demagnetiser. MS was measured at room temperature after each thermal demagnetisation step to assess possible mineralogical alterations.

In order to characterise the mineralogy and the magnetic properties, different rock-magnetic experiments were carried out using the Variable Field Translation Balance (MMVFTB) at the University of Burgos. Isothermal remanent magnetisation (IRM) acquisition and backfield coercivity experiments were carried out as well as hysteresis loops (±1 T) and Curie curves on bulk sample (~400 mg) for 4 (BR1) and 5 ashes (FU1), respectively. The thermomagnetic experiments were performed in air up to 700 °C and applying a field of 38 mT. Hysteresis loops allow the determination of magnetisation parameters: saturation magnetisation (M_s), remanence saturation magnetisation (M_{rs}) and coercive field (H_c). With these parameters and the remanence coercivity (H_{cr}), determined separately in a backfield experiment, the Day plot (Day et al., 1977) was used to study the grain size distribution of the samples.

4. Results

Initial NRM intensities in the ashes from *fumier* FU1 are between 7.4×10^{-4} and 8.2×10^{-5} Am^2 kg^{-1} while susceptibilities vary between 3.8×10^{-6} and 6.05×10^{-7} m^3 kg^{-1}. In the case of the BR1 site, the NRM$_0$ intensities are between 1.38×10^{-4} and 2.01×10^{-5} Am^2 kg^{-1}, and susceptibilities vary between 2.9×10^{-6} and 6.4×10^{-7} m^3 kg^{-1}. The mean NRM intensities and magnetic susceptibility values for both *fumiers* as well as their respective standard deviations are indicated in Table 1. As far as the ashes are concerned, the structure of the NRM demagnetisation diagrams is different among the samples from the two fires studied. The ashes corresponding to *fumier* FU1 are defined by high values of magnetisation and univectorial NRM demagnetisation diagrams (Fig. 3a and b). On the contrary, BR1 ashes display much more heterogeneous behaviour. Most of these specimens show lower values of magnetisation in comparison with FU1, and their orthogonal NRM demagnetisation diagrams exhibit multicomponent behaviour with anomalous directions (Fig. 3c–e).

There seems to be a direct relationship between the structure of the NRM orthogonal demagnetisation diagrams and the sample location within the fire. In the case of the bioturbated *fumier* BR1, the only samples with high intensities, univectorial and reliable (northwards) directional NRM diagrams are located on the edges of the structure, which seems to be unaffected by the burrow (e.g.: Fig. 2b and Fig. 3f). These samples are BR1-3, 7, 17, 18, 19, 20, 26, 29 and 31 and all but three (BR1-3, 21 and 29) are mostly located in the outer right side of the fumier (Fig. 2b). Interestingly, this observation also correlates well with the Koenigsberger ratio. This is a useful parameter in relation with the study of archaeological fires [$Q_n = \mathrm{NRM}/(\chi H)$ (*cf.* Stacey, 1967)], where χ is the magnetic susceptibility and H is the geomagnetic field strength. It provides an estimate of the efficiency of the NRM acquisition mechanism on the basis on the relationship between the induced and the remanent magnetisation. Most ashes

Table 1
Palaeomagnetic results obtained for the *fumiers* BR1 and FU1, including their corresponding Fisher (1953) statistical parameters. Columns from left to right: *n*: number of independently oriented samples taken into account in the calculation of the mean sample directions; *Dec.*: declination; *Inc.*: inclination; *k* and $\alpha 95$: precision parameter and 95 per cent confidence limit of characteristic remanent magnetisation, respectively. *NRM mean*: mean value of the natural remanent magnetisation; Mag. Susceptibility mean: mean value of the magnetic susceptibility; *Std. Deviation*: refers to standard deviation; Q_n *ratio*: Koenigsberger ratio. LC/LT (low-coercivity/low temperature); HC/HT (high coercivity/high temperature).

Fumier	*n*	Dec.	Inc.	*k*	$\alpha 95$	NRM mean ($Am^2\ kg^{-1}$)	NRM Std. Deviation	Mag. susceptibility mean ($m^3\ kg^{-1}$)	Mag. susceptibility Std. Deviation	Q_n ratio	Q_n ratio Std. Deviation
BR1[a]						5.16E-05	3.53E-05	1.52E-06	6.71E-07	0.99	0.82
BR1 [LC/LT component][b]	28	17.4	54.4	25.8	5.5	5.86E-05	3.63E-05	1.58E-06	7.41E-07		
BR1 [HC/HT component][b]	18	2.9	36.3	1.7	41.8						
BR1 [LC/LT component][c]	8	19.6	49.1	31.3	10.1	2.46E-05	7.28E-06	1.27E-06	8.00E-08		
BR1 [HC/HT component][c]	8	359.1	53.9	1.3	93						
FU1	22	336.8	52.8	43.8	4.7	1.94E-04	1.69E-04	2.00E-06	1.20E-06	3.27	0.99

[a] Including samples from the burrow.
[b] Excluding samples from the burrow.
[c] only samples from the burrow.

with multicomponent NRM demagnetisation diagrams and anomalous directions exhibit Q_n ratio values less than unity (Fig. 4a). Fig. 4a illustrates how FU1 ashes exhibit higher NRM intensity values than the ashes from the bioturbated *fumier* BR1 and two distinctive distributions can be observed when plotting their respective Q_n ratio values in a histogram, as in Fig. 4b. These values could seem low in comparison with those reported from volcanic rocks or other archaeomagnetic materials such as kilns, bricks or furnaces, between 1 and 100 (e.g. Gómez-Paccard et al., 2006; Catanzariti et al., 2008). However, they are in the range of burnt soils and hearths (e.g. Linford and Canti, 2001; Schnepp et al., 2004) and are very similar to the values obtained in analogous materials at El Mirón Cave -Cantabria, Northern Spain- (Carrancho and Villalaín, in press). Therefore, Q_n ratio values from FU1 (mean value = 3.27) might well correspond with a stable thermoremanent origin of NRM.

The magnetic properties of these ashes are very similar in terms of mineral composition, grain size and concentration. Hysteresis loops (expressed on a mass-specific basis and corrected for the paramagnetic fraction) and progressive IRM acquisition curves in both *fumiers* reach saturation at fields around 200–300 mT, indicating the dominance of a low-coercivity mineral (Fig. 5a and b). The intensity of magnetisation is twice in the *in situ* fumier FU1, although of the same order of magnitude. According to these results and the thermomagnetic (*J*–*T*) curve analyses which show Curie temperatures of 585–600 °C, the main magnetic carrier in the ashes from both *fumiers* is magnetite or partially maghemitized magnetite. This mineralogical identification agrees well with the thermal demagnetisation NRM plots with maximum unblocking temperatures (T_{UB}) comprised between 580 and 615 °C (e.g.: Fig. 3a and e). The magnetisation (M_{rs}/M_s) and coercivity (H_{cr}/H_c) ratios for representative ash samples from both *fumiers* have been plotted on a Day plot (Day et al., 1977; Fig. 6), including the mixing curves determined by Dunlop (2002) for magnetite. All samples plot in the pseudo-single domain (PSD) area, more or less clustered, which suggests that the grain size distribution in this facies is quite similar. These magnetic properties agree also well with previous mineral magnetic data from the Neolithic *fumiers* at the site (Carrancho et al., 2009). Furthermore, the similarity in the magnetic properties of the ashes is striking, regardless of their colour variations and degree of preservation. In addition, the heating and cooling curves of the thermomagnetic curves for both samples are very similar, indicating that the magnetic minerals are stable to 700 °C (Fig. 5a and b). The AMS analyses (Fig. 7a–f) show a weak anisotropy with values of P' (degree of anisotropy) of about 0.01 and dispersed directions. However, most ash samples from both *fumiers* exhibit susceptibility ellipsoids of predominantly oblate shape ($T > 0$ in Fig. 7b and d) with the minimum axis (k_3) oriented more or less parallel to the vertical, contained within the 95% confidence ellipses (Fig. 7a and c). In both cases, this anisotropy is probably due to compaction effects. Nevertheless, the samples corresponding to the BR1 burrow (Fig. 7e and f) display more scattered axes directions and heterogeneous shapes. This magnetic fabric reflects mechanical reworking induced by bioturbation.

The characteristic remanent magnetisations (*ChRM*) and their statistical parameters were calculated using linear regression and Fisher (1953) statistics. The characteristic component in FU1 was calculated considering the only directional component present in the NRM (Fig. 3a and b). In the case of the BR1 site, most samples exhibit multicomponent behaviour and the *ChRM* was systematically calculated above 300 °C or 15–20 mT, following the range considered in FU1 and taking into account that both *fumiers* exhibit similar magnetic properties. The directional results obtained from both *fumiers* are represented in equal-area projections together with their mean directions in Fig. 8a and b. Although samples from *fumier* FU1 are well-grouped defining with high precision a mean direction at the 95% confidence level ($\alpha 95$), samples from BR1 are randomly distributed on the stereogram. In the latter case, this behaviour can only be explained because the structure is no longer *in situ*. Only those samples corresponding to the edges of the structure and that at the macroscopic scale do not show evidence of mechanical disturbance (black circles in Fig. 8b), and are relatively clustered on the stereo-plot.

An interesting aspect with regard to the bioturbation of *fumier* BR1 is the comparison of the mean directions determined for the first (low-coercivity) component of this fire, considering samples from inside and outside the burrow (Table 1 and Fig. 8c). Except for the few samples mentioned before, the high-coercivity components (>15–20 mT) of most BR1 ashes exhibit random directions as a consequence of the bioturbation (Fig. 8b). However, the low-coercivity component of the samples from the burrow displays similar directions compared with the rest of the ashes of this *fumier*, and both mean directions are contained within their respective confidence circles, $\alpha 95$ (Fig. 8c and Table 1). This implies that this first component was acquired after the mechanical alteration, and most probably is of viscous origin. Carrancho et al. (2009) showed that the low-coercivity component of the ashes in some Neolithic *fumiers* can acquire a viscous magnetisation with coercive fields of 12–14 mT, similarly to that observed in BR1 ashes (Fig. 3c and d).

5. Discussion

Nowadays, studies about post-depositional processes of archaeological cave fires represent one of the major issues in geoarchaeology. Systematic studies carried out since the 1990s at several Mediterranean caves have showed the variety and complexity of syn- and post-depositional processes that archaeological cave fires may undergo. Most of these works have been tackled from a geochemical

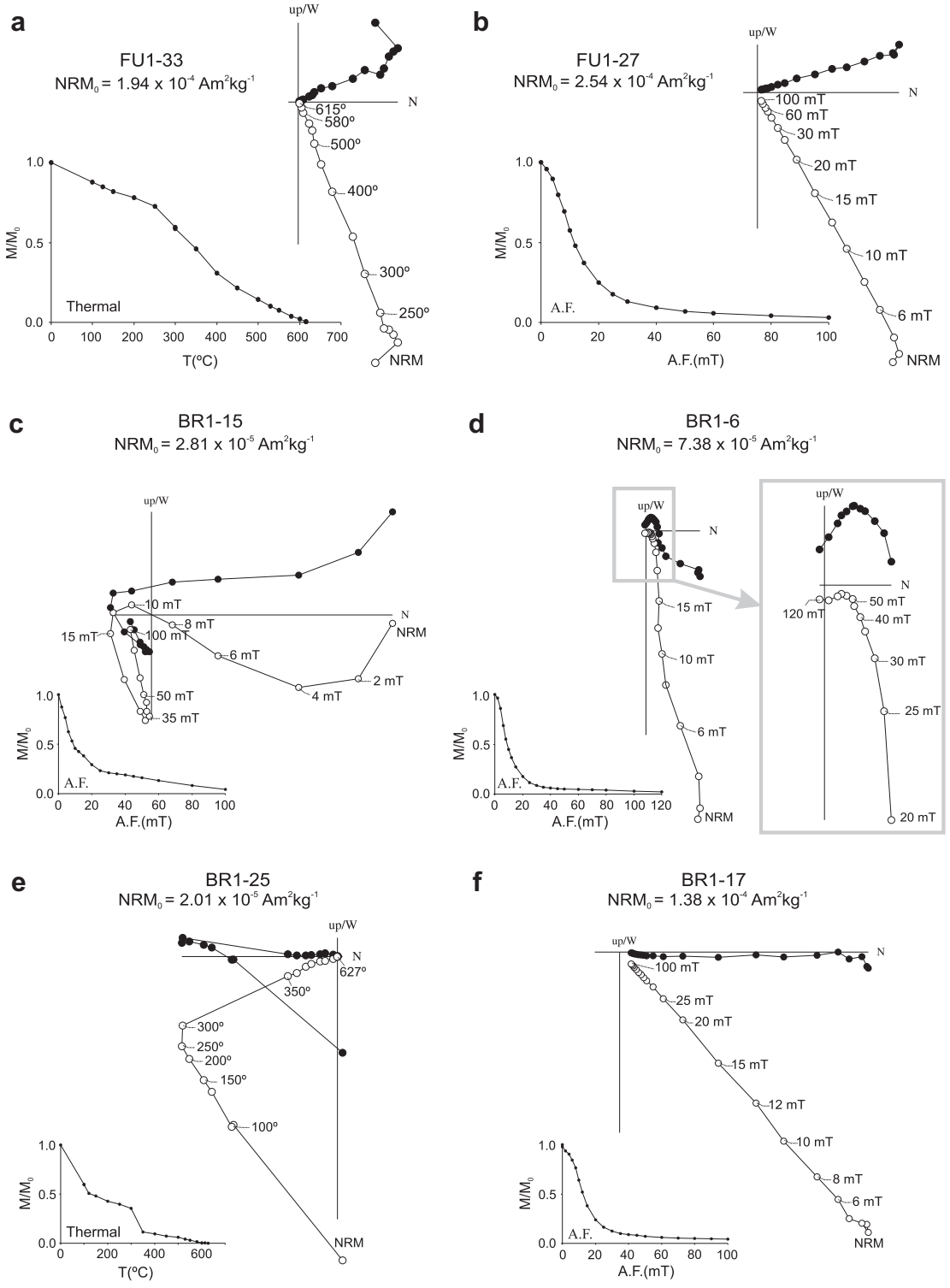

Fig. 3. Orthogonal NRM demagnetisation plots of representative ash samples from (a and b) FU1 site and (c–f) BR1 site. Solid (open) circles show projections of vector endpoints onto the horizontal (vertical) plane. The intensity (NRM_0), code and demagnetisation spectra are indicated for each sample. The decay curves represent the normalized intensity (M/M_0) after their respective demagnetisation step.

viewpoint, focusing on the study of the sequential mineralogical transformations that calcite, as the major constituent of ash, undergo during diagenesis (e.g. Schiegl et al., 1996; Karkanas et al., 1999, 2000; Weiner et al., 2002). Chemical transformations in archaeological fires also involve calcifications, phosphatization, or leaching, among other processes. On the other hand, post-depositional processes also comprise physical alteration of sediments (i.e. mechanical reworking). Regardless of the agents responsible, these effects may imply the translocation of bones, microartefacts or paleobotanical remains, with the subsequent stratigraphic implications that it entails.

In recent years there has been a growing interest in the study of taphonomic and post-depositional processes in anthropogenic deposits, especially through soil micromorphology analysis

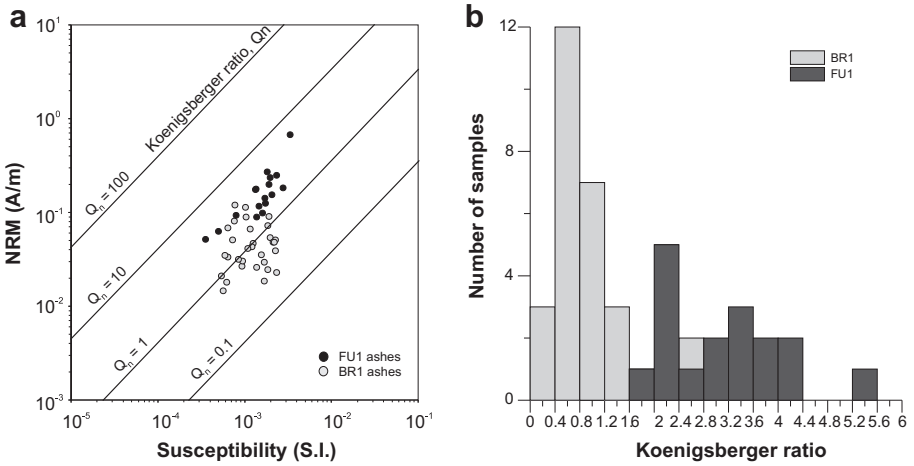

Fig. 4. (a) Bi-plot of NRM intensity *vs*. magnetic susceptibility for the ashes from both *fumiers*, indicating isolines of equal Koenigsberger ratio (Q_n). (b) Histogram with the Q_n values corresponding to the ash samples plotted in (a).

(Karkanas, 2006; Polo Díaz and Fernández Eraso, 2010). The main syn- and post-depositional effects of physical character observed in this type of deposits include a major reduction in the original volume of ashes during burning, mixing and/or truncation of microfacies, washing of sediments, compaction, and bioturbation. The taphonomy of stabling sequences is complex, considering the numerous geochemical and/or physical processes involved. Although geochemical and mineralogical studies have had a longer tradition in these contexts, identification of physical alterations has mainly been based on macroscopic and/or microscopic observations. The most common way to identify post-depositional alterations in these fires is by observing the geometry, thickness and lateral extension of ashes and rubefacted facies exposed on stratigraphic profiles. The lateral continuity of the microfacies, the presence of the rubefaction underlying the ashes, and a regular geometry and shape of the fire, are good indicators of its preservation.

In this case study, it is clear that the mechanical disturbance of the ashes caused by bioturbation in *fumier* BR1 has completely distorted the original record of the geomagnetic field. Otherwise, the directions should point northwards instead of being anomalous, showing a random distribution on the stereo-plot (Fig. 8b). However, the archaeomagnetic directions obtained in *fumier* FU1 are statistically well-grouped, confirming that this fire is well-preserved and retains its physical integrity (Fig. 8a). When these anthropogenic fires physically preserve their primary position, a set of common magnetic features have been observed which can be

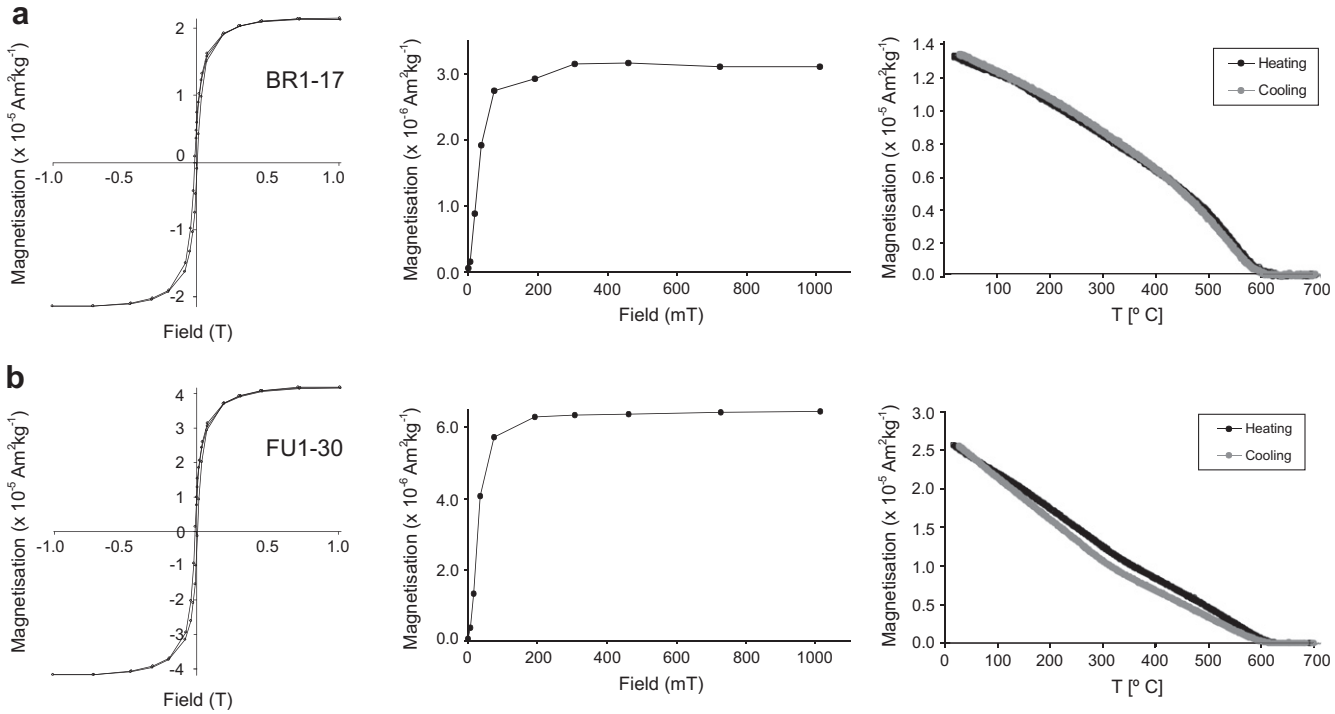

Fig. 5. (a–b) Representative examples of different rock-magnetic experiments of two ashes from BR1 and FU1 sites, respectively. Diagrams from left to right correspond to a hysteresis loop (±1 T), a progressive acquisition isothermal remanent magnetisation (IRM) curve and a thermomagnetic (Curie) curve. The sample code and magnetisation values for each specimen are indicated. Heating (black) and cooling (grey) cycles are shown according to the legend.

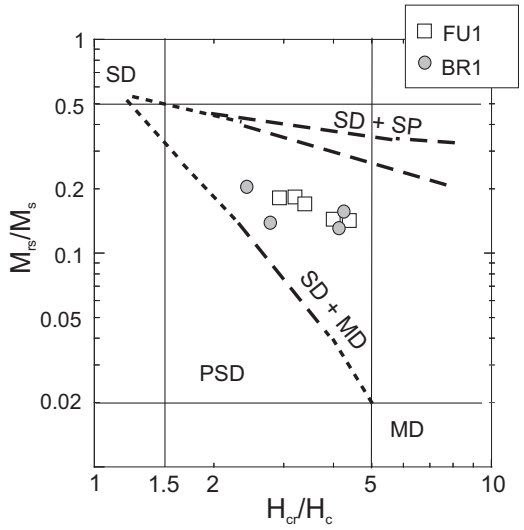

Fig. 6. M_{rs}/M_s versus H_{cr}/H_c logarithmic plot of representative ash samples from both *fumiers* according to the legend. The dashed lines represent mixing curves taken from Dunlop (2002) for mixtures of single-domain (SD) with multidomain (MD) or superparamagnetic (SP) magnetite particles.

used as indicators of the absence of post-depositional alterations. These are: i) univectorial NRM orthogonal demagnetisation diagrams in the ashes, ii) Q_n ratio values higher than one, indicating that the mechanism of magnetisation is a TRM or a partial TRM (p-TRM); and iii) a good clustering of characteristic directions showing an statistically well-defined mean archaeomagnetic direction. The occurrence of these magnetic features within a cave fire indicates that it is *in situ*. Logically, this information must be also combined with the analysis of the macroscopic features of the fires and application of other techniques if available.

According to the results observed in *fumier* BR1, reworked ashes show unstable and multicomponent NRM demagnetisation diagrams. The NRM of these samples is at least composed by: *i)* a high coercivity/unblocking temperature component ($H_c > 15$ mT/$T_{UB} > 300$ °C) carried by grains with long relaxation times which have undergone reorientation due to mechanical alteration; and *ii*) a viscous component with low-coercivities/unblocking temperatures carried by grains with short relaxation times (lower than the age of the mechanical alteration) which were remagnetized toward north (e.g.: Fig. 3e and Fig. 8c). If the reworking of the ashes occurred at a smaller scale than the sample size, additional components might be observed (Fig. 3c and d).

In addition, the intensity of magnetisation in reworked ashes is substantially lower than those from an *in situ* fire. Most Q_n ratio values are less than unity, and depending on the preservation degree of the structure, it will not be possible to obtain a mean archaeomagnetic direction statistically representative. Mechanical alterations induced by bioturbation may affect an archaeological cave fire with deeper and even imperceptible effects in the material than those seen macroscopically. Thus, if sampling covers the whole fire area, the vectorial analysis of archaeomagnetic samples may elucidate which specific parts of the structure were not affected by mechanical alteration. This is the case of the few ash samples mostly located near the edges of the BR1 site (e.g.: Fig. 3f) which seem to preserve reasonably well their original position, as they are relatively clustered in the stereo-plot (black circles in Fig. 8b).

Beyond the visual evidence of mechanical disturbance in the ashes, the Q_n ratio is a good indication of preservation of TRM. Samples that are not pure ash and are mixed with unburnt sediment, such as those from BR1, display the lowest Q_n ratio values, due to having lost their TRM through disorganization of the magnetic moments of their ferromagnetic grains. The vector sum of these magnetic moments results in a lower value of the total magnetisation. The magnetic susceptibility, however, which does not depend

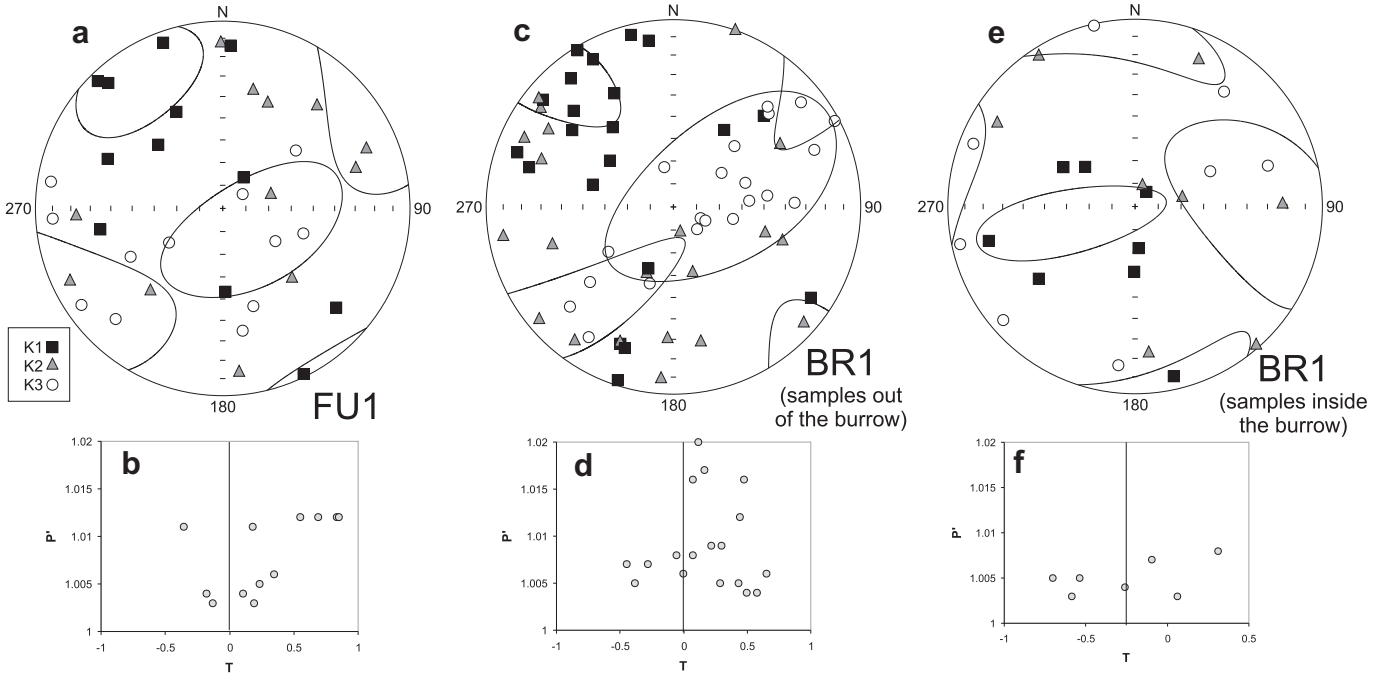

Fig. 7. (a–f) Anisotropy of magnetic susceptibility (AMS) results in FU1 (a–b), BR1 samples out of the burrow (c–d) and BR1 samples inside the burrow (e–f). (a, c and e) Equal-area projections showing the *in situ* directions of principal axes of susceptibility ellipsoid: maximum (k_1), intermediate (k_2) and minimum (k_3) directions. The 95% confidence ellipses are indicated. (b, d and f) The corresponding diagrams of P' (corrected anisotropy degree) *vs.* T (shape parameter) according to Jelinek (1981) are also indicated.

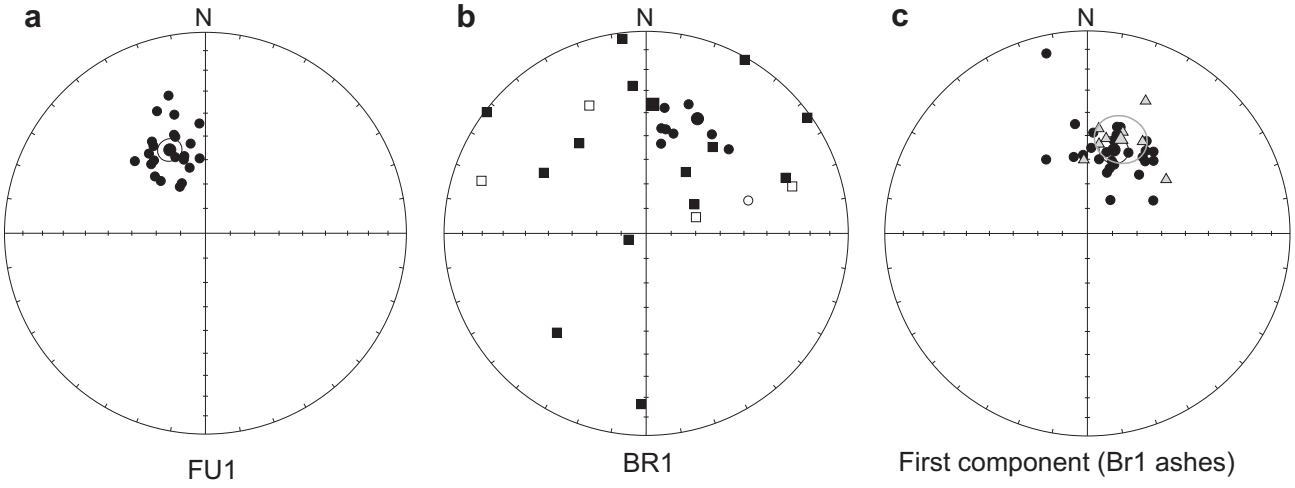

Fig. 8. (a–c) Equal-area projections showing the results of *ChRM* directions obtained for (a) FU1; (b) BR1 and (c) the low-coercivity component of BR1 ashes from inside (grey triangles) and outside the burrow (black circles). The mean directions (large icons) together with the $\alpha 95$ confidence error for the FU1 are indicated. Black circles in (b) represent the ashes corresponding to the edges of the structure and the squares the rest of the collection (see text for explanation). The mean archaeomagnetic direction and Fisherian statistical parameters obtained for FU1 are: Declination = 336.8°; Inclination = 52.8°; k = 43.8; $\alpha 95$ = 4.7°. See also Table 1.

on the orientation of magnetic grains, excluding the magnetic anisotropy effects, is high, thus yielding low values of Q_n ratio.

Any mechanical alteration of the sediment changes the archaeomagnetic direction originally recorded during the cooling of the material. Ferromagnetic grains contained within these facies should preserve the original geomagnetic field direction if no post-burning process has affected the combustion structure. The scattering of most samples from BR1 are due to post-cooling movements rather than due to a low intensity of heating that would not have locked in the remanence. In spite of the low Q_n ratio values, the high degree of reversibility of thermomagnetic curves (Fig. 5a) shows that they were well heated.

Geochemical transformations are more difficult to identify, but mineral magnetic methods can also provide useful information about potential post-depositional processes. The fact that the magnetic mineralogy is very similar in both structures suggests that they have undergone similar combustion and/or conservation processes from the geochemical point of view.

Considering that these are non-lithified materials and that the magnetisation resides in micrometric particles with a certain degree of mobility, the vectorial analysis of archaeomagnetic directions allows assessment of the preservation state of a fire and its *in situ* character. In archaeomagnetic studies, any process that may cause directional distortions in a studied feature, no matter how minimal, is critical. Nevertheless, if post-depositional processes are not severe and do not cause major displacements among the archeological artifacts within the stratigraphy, there is no reason why the cultural interpretation of the archeological record should be adversely affected.

6. Conclusion

Archaeomagnetic and rock-magnetic analysis represent powerful research tools to identify and evaluate potential post-depositional processes in archaeological cave fires. Comparison of the archaeomagnetic directions recorded in two differentially preserved cave fires has allowed determination of a common set of magnetic features which can be used as a criterion to assess when a burning feature is *in situ* and mechanically undisturbed. A reworked archeological fire is defined by: *i)* multicomponent structure of the NRM demagnetisation diagrams in ashes with anomalous directions; *ii)* Q_n ratio values below unity implying that the samples do not carry a TRM; and *iii)* scattered archaeomagnetic directions. An *in situ* archaeological fire is defined by: *i)* a stable single component of NRM with consistent direction; *ii)* Q_n ratio above unity, indicative of a TRM; and *iii)* a good clustering of characteristic directions defining an statistically representative mean archaeomagnetic direction. This information must be combined with field (macroscopic) observations.

Acknowledgments

This work has been carried out with the financial support of the Spanish Ministry of Science and Technology (CGL2009-10840) and Junta de Castilla y León (BU004A09). Ángel Carrancho acknowledges the financial support given by Fundación del Patrimonio Histórico de Castilla y León. Special gratitude is devoted to the archaeologists working at El Mirador Cave for their great help in field-work, as well as the editors of this special issue for their invitation to make this contribution.

We appreciate the reviews of Maria Luisa Osete and an anonymous reviewer whose constructive comments considerably improved the paper.

References

Angelucci, D.E., Boschian, G., Fontanals, M., Pedrotti, A., Vergès, J.M., 2009. Shepherds and karst: the use of caves and rock-shelters in the Mediterranean region during the Neolithic. World Archaeology 41 (2), 191–214.

Arsuaga, J.L., Bermúdez de Castro, J.M., Carbonell, E., 1997. The Sima de los Huesos hominid site. Journal of Human Evolution 33, 105–421.

Bermúdez de Castro, J.M., Carbonell, E., Arsuaga, J.L., 1999. The Gran Dolina site: TD6 Aurora Stratum (Atapuerca, Burgos, Spain). Journal of Human Evolution 37, 309–700.

Bonifay, E., 1956. Les sédiments détritiques grossiers dans le remplissage des grottes—méthode d'étude morphologique et statistique. L'Anthropologie 60, 447–461.

Boschian, G., 1997. Sedimentology and soil micromorphology of the late Pleistocene and early Holocene deposits of Grotta dell'Edera (Trieste Karst, NE Italy). Geoarchaeology 12 (3), 227–249.

Boschian, G., Montagnari-Kokelj, E., 2000. Prehistoric shepherds and caves in Trieste Karst (northeastern Italy). Geoarchaeology 15, 332–371.

Brochier, J.E., 1983. Combustion et parcage des herbivores domestiques. Le point de vue du sédimentologue. Bulletin de la Société Préhistorique Française 80 (5), 143–145.

Brochier, J.E., Villa, P., Giacomarra, M., 1992. Shepherds and sediments: geo-ethnoarchaeology of pastoral sites. Journal of Anthropology and Archaeology 11, 47–102.

Cabanes, D., Burjachs, F., Expósito, I., Rodríguez, A., Allué, E., Euba, I., Vergès, J.M., 2009. Formation processes through archaeobotanical remains: the case of the Bronze Age levels in El Mirador cave, Sierra de Atapuerca, Spain. Quaternary International 193, 160–173.

Cáceres, I., Lozano, M., Saladié, P., 2009. Evidence for Bronze Age cannibalism in El Mirador Cave (Sierra de Atapuerca, Burgos, Spain). American Journal of Physical Anthropology 133 (3), 899–917.

Carbonell, E., Bermúdez de Castro, J.M., Parés, J.M., Pérez-González, A., Cuenca-Bescós, G., Ollé, A., Mosquera, M., Huguet, R., van der Made, J., Rosas, A., Sala, R., Vallverdú, J., García, N., Granger, D.E., Martinón-Torres, M., Rodríguez, X.P., Stock, G.M., Vergès, J.M., Allué, E., Burjachs, F., Cáceres, I., Canals, A., Benito, A., Díez, C., Lozano, M., Mateos, A., Navazo, M., Rodríguez, J., Rosell, J., Arsuaga, J.L., 2008. The first hominin of Europe. Nature 452, 465–469.

Carrancho, Á., Villalaín, J.J., Angelucci, D.E., Dekkers, M.J., Vallverdú, J., Vergès, J.M., 2009. Rock-magnetic analyses as a tool to investigate archaeological fired sediments. A case study of Mirador cave (Sierra de Atapuerca, Spain). Geophysical Journal International 179, 79–96.

Carrancho, Á., Villalaín, J.J., in press. Preliminary archaeomagnetic and rock-magnetic results from the Holocene fire lenses in El Mirón Cave (Ramales de la Victoria, Spain). In: Straus, L.G., González-Morales, R.M. (Eds.), El Mirón Cave. Background, Stratigraphy, Sedimentology and the Post-Paleolithic Levels, vol. 1. New Mexico University Press, USA, 17 pp. ISBN: 978 0 8263 5148 7.

Catanzariti, G., McIntosh, G., Monge Soares, A.J., Díaz-Martínez, E., Kresten, P., Osete, M.L., 2008. Archaeomagnetic dating of a vitrified wall at the Late Bronze Age settlement of Misericordia (Serpa, Portugal). Journal of Archaeological Science 35, 1399–1407.

Day, R., Fuller, M.D., Schmidt, V.A., 1977. Hysteresis properties of titanomagnetites grain size and composition dependence. Physics of the Earth and Planetary Interiors 13, 260–266.

Dunlop, D.J., 2002. Theory and application of the Day plot (Mrs/Ms versus Hcr/Hc) 2. Application to data for rocks, sediments, and soils. Journal of Geophysical Research 107. doi:10.1029/2001JB000487.

Farrand, W.R., 1975. Sediment analysis of a prehistoric rockshelter: the Abri Pataud. Quaternary Research 5, 1–26.

Fisher, R.A., 1953. Dispersion on a sphere. Proceedings, Royal Society of London A 217, 295.

Goldberg, P., Sherwood, S.C., 2006. Deciphering human prehistory through the geoarcheological study of cave sediments. Evolutionary Anthropology 15, 20–36.

Gómez-Paccard, M., et al., J. Archaeological Working Group, 2006. A catalogue of Spanish archaeomagnetic data. Geophysical Journal International 166, 1125–1143.

Herries, A.I.R., 2009. New approaches for integrating palaeomagnetic and mineral magnetic methods to answer archaeological and geological questions on Stone Age sites. In: Fairbrain, A., O'Conner, S., Marwick, B. (Eds.), Terra Australis 28-New Directions in Archaeological Science. The Australian National University Press, Canberra, Australia, pp. 235–253 (Chapter 16).

Herries, A.I.R., Fisher, E.C., 2010. Multidimensional GIS modelling of magnetic mineralogy as a proxy for fire use and spatial patterning: evidence from the Middle Stone Age bearing sea cave of Pinnacle Point 13B (Western Cape, South Africa). Journal of Human Evolution 59, 306–320.

Jelinek, V., 1981. Characterization of the magnetic fabric of rocks. Tectonophysics 79, 63–67.

Karkanas, P., 2006. Late Neolithic household activities in marginal areas: the micromorphological evidence from the Kouveleiki caves, Peloponnese, Greece. Journal of Archaeological Science 33 (11), 1628–1641.

Karkanas, P., 2010. Preservation of anthropogenic materials under different geochemical processes: a mineralogical approach. Quaternary International 214, 63–69.

Karkanas, P., Kyparissi-Apostolika, N., Bar-Yosef, O., Weiner, S., 1999. Mineral assemblages in Theopetra, Greece: a framework for understanding diagenesis in a prehistoric cave. Journal of Archaeological Science 26, 1171–1180.

Karkanas, P., Bar-Yosef, O., Goldberg, P., Weiner, S., 2000. Diagenesis in prehistoric caves: the use of minerals that form in situ to assess the completeness of the archaeological record. Journal of Archaeological Science 27, 915–929.

Lanos, Ph., Kovacheva, M., Chauvin, A., 1999. Archaeomagnetism, methodology and applications: implementation and practice of the archaeomagnetic method in France and Bulgaria. European Journal of Archaeology 2, 65–392.

Linford, N.T., Canti, M.G., 2001. Geophysical Evidence for fires in antiquity: preliminary results from an experimental study. Archaeological Prospection 8, 211–225.

Martín, P., Rosell, J., Vergès, J.M., 2009. The exploitation of faunal resources in the Neolithic of the Sierra de Atapuerca (Burgos): levels 19 and 20 of the Cueva de El Mirador. Trabajos de Prehistoria 66 (2), 7–92.

Polo Díaz, A., Fernández Eraso, J., 2010. Same anthropogenic activity, different taphonomic processes: a comparison of deposits from Los Husos I and II (Upper Ebro Basin, Spain). Quaternary International 214, 82–97.

Schiegl, S., Goldberg, P., Bar-Yosef, O., Weiner, S., 1996. Ash deposits in Hayonim and Kebara Caves, Israel: macroscopic, microscopic and mineralogical observations, and their archaeological implications. Journal of Archaeological Science 23, 763–781.

Schnepp, E., Pucher, R., Reinders, J., Hambach, U., Soffel, H., Hedley, I., 2004. A German catalogue of archaeomagnetic data. Geophysical Journal International 157, 64–78.

Shahack-Gross, R., Marshall, F., Weiner, S., 2003. Geo-ethnoarchaeology of pastoral sites: the identification of livestock enclosures in abandoned Maasai settlements. Journal of Archaeological Science 30, 439–459.

Stacey, F.D., 1967. The koenigsberger ratio and the nature of thermoremanence in igneous rocks. Earth and Planetary Sciences Letters 2, 67–68.

Stuiver, M., Reimer, P.J., Reimer, R.W., 2005. CALIB 5.0. [www program and documentation].

Vergés, J.M., Allué, E., Angelucci, D.E., Cebrià, A., Díez, C., Fontanals, M., Manyanós, A., Montero, S., Moral, S., Vaquero, M., Zaragoza, J., 2002. La Sierra de Atapuerca durante el Holoceno: datos preliminares sobre las ocupaciones de la Edad del Bronce en la cueva de El Mirador (Ibeas de Juarros, Burgos). Trabajos de Prehistoria 59 (1), 107–126.

Vergés, J.M., Allué, E., Angelucci, D., Burjachs, F., Carrancho, A., Cebrià, A., Expósito, I., Fontanals, M., Moral, S., Rodríguez, A., Vaquero, M., 2008. Los niveles neolíticos de la cueva de El Mirador (Sierra de Atapuerca, Burgos): nuevos datos sobre la implantación y el desarrollo de la economía agropecuaria en la submeseta norte. In: Hernández, M., Soler (Eds.), Actas del IV Congreso del Neolítico Peninsular. Museo Arqueológico de Alicante, Alicante, Spain, pp. 418–427.

Weiner, S., Goldberg, P., Bar-Yosef, O., 1993. Bone preservation in Kebara Cave, Israel using on-site Fourier transform infrared spectroscopy. Journal of Archaeological Science 20, 613–627.

Weiner, S., Goldberg, P., Bar-Yosef, O., 2002. Three-dimensional distribution of minerals in the sediments of Hayonim cave, Israel: diagenetic processes and archaeological implications. Journal of Archaeological Science 29, 1289–1308.

Weiner, S., Berna, F., Cohen-Ofri, I., Shahack-Gross, R., Albert, R.M., Karkanas, P., Meignen, L., Bar-Yosef, O., 2007. Mineral distributions in Kebara Cave: diagenesis and its affect on the archaeological record. In: Bar- Yosef, O., Meignen, L. (Eds.), Kebara Cave, Mt. Carmel, Israel: The Middle and Upper Paleolithic Archaeology. American School of Prehistoric Research Bulletin 49. Peabody Museum of Archaeology and Ethnology, Harvard University, Cambridge, pp. 131–146.